https://doi.org/10.5194/bg-2019-448
Preprint. Discussion started: 19 November 2019

Biogeosciences Discussions
Open Access
EGU

Macroalgal metabolism and lateral carbon flows create extended atmospheric CO_2 sinks

Kenta Watanabe[1], Goro Yoshida[2], Masakazu Hori[2], Yu Umezawa[3], Hirotada Moki[1], and Tomohiro Kuwae[1]

[1]Coastal and Estuarine Environment Research Group, Port and Airport Research Institute, 3-1-1 Nagase, Yokosuka 239-0826, Japan
[2]National Research Institute of Fisheries and Environment of Inland Sea, Japan Fisheries Research and Education Agency, 2-17-5 Maruishi, Hatsukaichi 739-0452, Japan
[3]Department of Environmental Science on Biosphere, Tokyo University of Agriculture and Technology, 3-5-8 Saiwai-cho, Fuchu, Tokyo 183-8509, Japan

Correspondence to: Kenta Watanabe (watanabe-ke@p.mpat.go.jp)

Abstract. Macroalgal beds have drawn attention as one of the vegetated coastal ecosystems that act as atmospheric CO_2 sinks. Although macroalgal metabolism as well as inorganic and organic carbon flows are important pathways for CO_2 sequestration by macroalgal beds, the relationships between macroalgal metabolism and associated carbon flows are still poorly understood. In the present study, we investigated carbon flows, including air–water CO_2 exchange and budgets of dissolved inorganic carbon, total alkalinity, and dissolved organic carbon (DOC) in a temperate macroalgal bed during productive months of the year. To assess the key mechanisms of CO_2 sequestration by the macroalgal bed, we estimated macroalgal metabolism and lateral carbon flows using a field-bag method, a degradation experiment, and mass balance modelling over a diurnal cycle. Our results showed that macroalgal metabolism and lateral carbon flows driven by water exchange affected air–water CO_2 exchange in the macroalgal bed and the surrounding waters. Macroalgal metabolism caused overlying waters to contain low concentrations of CO_2 and high concentrations of DOC that were efficiently exported offshore from the macroalgal bed. The exported water lowered CO_2 concentrations in the offsite surface water and enhanced atmospheric CO_2 uptake. Our findings suggest that macroalgal beds in habitats associated with high water exchange rates can create extensive CO_2-sinks around them.

1 Introduction

Vegetated coastal ecosystems provide a variety of ecosystem functions that support diverse biological communities and biogeochemical processes. Recent recognition of the carbon sequestration function of these ecosystems has led to the development of Blue Carbon strategies for mitigating the adverse effects of global climate change via conservation and restoration of these ecosystems (Nellemann et al., 2009; Duarte et al., 2013; Macreadie et al., 2019).

Carbon flows that sequester atmospheric CO_2 in marine ecosystems over timescales of at least several decades are crucial for the mitigation of climate change (McLeod et al., 2011; Macreadie et al., 2019). Organic carbon burial in sediments is one

https://doi.org/10.5194/bg-2019-448
Preprint. Discussion started: 19 November 2019

of the most important pathways to sequester carbon for a long time (Nellemann et al., 2009; Miyajima et al., 2019). Evaluation of the carbon sequestration function of vegetated coastal ecosystems has thus been focused on saltmarshes, seagrasses, and mangroves, which develop their own organic-rich sediments (Macreadie et al., 2019). In contrast, beds of macroalgae have been assumed to have limited capacity to sequester carbon because they generally settle on hard strata such as rocks and artificial structures (Krause-Jensen et al., 2018). Organic matter produced by macroalgae is more labile than that produced by vascular plants (Trevathan-Tackett et al., 2015) and hence is efficiently utilized by consumers and decomposers (Duarte, 1995). However, macroalgal beds are estimated to be the most extensive vegetated coastal habitats (3.5 million km^2) in the global ocean, and their global net primary production (1521 Tg-C yr^{-1}) is comparable to that of other vegetated coastal habitats (Krause-Jensen and Duarte, 2016; Duarte, 2017; Raven, 2018). Macroalgal beds therefore have the potential to sequester substantial amounts of carbon in marine ecosystems.

Other processes in addition to organic carbon burial in on-site sediments must exist for macroalgae to contribute to atmospheric CO_2 sequestration. Recent studies have proposed that a large fraction of macroalgal production is exported to other vegetated coastal ecosystems, shelves, and the deep sea, where organic carbon derived from macroalgae can be stored for a long time (Krause-Jensen and Duarte, 2016; Krause-Jensen et al., 2018).

Macroalgal beds export about 43 % of their production both as dissolved organic carbon (DOC) and particulate organic carbon (POC) (Krause-Jensen and Duarte, 2016). A first-order estimate has suggested that 33 % of the flux of DOC derived from macroalgae is exported below the mixed layer, where it contributes to carbon sequestration (Bauer and Druffel, 1998; Krause-Jensen and Duarte, 2016). Because the proportion of DOC that persists for a long time is estimated to be higher than that of POC (15 %) (Krause-Jensen and Duarte, 2016), DOC production, export, and degradation are believed to be significant processes for carbon sequestration. Although the production of refractory DOC by macroalgae is one of the important factors that impacts carbon sequestration, there are few relevant data (e.g., Wada et al., 2008; Wada and Hama, 2013). The long residence time of refractory DOC in the water column increases the probability that it reaches depths below the mixed layer.

The dissolved constituents of the carbonate system must be assessed to quantify the effect of community metabolism on air–water CO_2 exchange (Macreadie et al., 2019; Tokoro et al., 2019). The high rates of macroalgal photosynthesis and respiration change dissolved inorganic carbon (DIC) concentrations. Calcification and dissolution of associated organisms modify the total alkalinity (TAlk) and DIC. Physical parameters and the balance of the carbonate system decide the magnitude of the air–water CO_2 exchange (Tokoro et al., 2019). Indeed, some previous studies have shown that macroalgal beds act as sinks for atmospheric CO_2 (Delille et al., 2009; Ikawa and Oechel, 2015; Koweek et al., 2017). However, the effects of macroalgal metabolism on the carbonate system in both macroalgal beds and adjacent water bodies have not been quantified.

Despite the importance of dissolved carbon flows as CO_2 sequestration pathways, little attention has been paid to assessing the related carbon budgets in macroalgal beds. In this study, we assessed carbon flows, including air–water CO_2 exchange and changes of DIC, TAlk, and DOC in a temperate macroalgal bed during productive periods (winter). To

https://doi.org/10.5194/bg-2019-448
Preprint. Discussion started: 19 November 2019


Biogeosciences Discussions

quantify macroalgal metabolism and dissolved carbon flows, we used a field-bag method, a degradation experiment, and mass balance modelling. In the present study, we focused on sargassaceous algae because this macroalgae is the dominant group in temperate regions (e.g., Yoshida et al., 2019). Our goals were to quantify the contribution of macroalgal beds to CO_2 sequestration and to investigate the responsible mechanisms on a daily timescale.

2 Materials and methods

2.1 Study site and sample collection

This study was conducted in the coastal waters of Heigun Island (33°46'1.7"N, 132°15'24.3"E) in the western Seto Inland Sea in Japan (Fig. 1). The macroalgal bed at the study site is dominated by sargassaceous algae (Figs. S1 and S2 in the Supplement). The surface area of the macroalgal bed is 1.44 ha, and the macroalgal habitat is located at a depth shallower than 5 m (mean depth, 2.0 m). There is no significant freshwater input from the island.

Field surveys were conducted in February and March of 2019 in the macroalgal bed and the adjacent water bodies in order to consider the temporal variations of biotic and abiotic conditions. These months are the most productive period of sargassaceous algae around this study site (Yoshida et al., 2001). Surface water samples for analyses of DIC, TAlk, and DOC were collected from a research vessel three times during the daytime in both February and March of 2019 at five stations (H1–H5) (Fig. 1). Four stations (H1–H4) inside the macroalgal bed were set at equal intervals between the ends of the bed in order to assess average conditions. Station H5 was established at an offshore site. Samples for DIC and TAlk were dispensed into 250-mL Schott Duran bottles and preserved with mercuric chloride (200 µL per bottle) to prevent DIC changes due to biological activity. Water samples for DOC analysis were filtered through 0.2-µm polytetrafluoroethylene filters (DISMIC–25HP; Advantec, Durham, NC, USA) into precombusted (450 °C for 2 h) 50-ml glass vials and frozen at −20 °C until analysis. At each station, the salinity, temperature, and chlorophyll fluorescence of the surface water was recorded with a RINKO-Profiler (ASTD102, JFE Advantech, Nishinomiya, Japan).

Field bag experiments (e.g., Wada et al., 2007; Towle and Pearse, 1973) were conducted to quantify the changes of DIC, TAlk, and DOC by macroalgae in February and March of 2019. We selected *Sargassum horneri* as a subject species because sufficient amounts of *S. horneri* were present in a zone suitable for the experiments. The entire thallus of an individual *S. horneri* was covered with a plastic bag containing the ambient seawater. The open end of the bag was tied at the algal stipe by scuba divers. Triplicate transparent and dark bags were set up to measure the changes of dissolved constituents due to macroalgal metabolism (Fig. S3 in the Supplement). To assess the effect of phytoplankton, a set of transparent and dark bags were filled with ambient seawater that contained no macroalgae. These bags served as control bags. Water samples from the bags were collected just after the start of the experiment and about 4 h later through a Tygon® tube by using a hand-held vacuum pump. The collected water samples were preserved with mercuric chloride (vide supra). After the experiments, the volume of seawater and the wet weight of the macroalgae were measured. At the beginning and end of the experiments, the salinity, temperature, and chlorophyll fluorescence of the surface water were recorded with a RINKO-Profiler (ASTD102,

https://doi.org/10.5194/bg-2019-448
Preprint. Discussion started: 19 November 2019

JFE Advantech, Nishinomiya, Japan). Photosynthetic photon flux was measured with a photon flux sensor (DEFI-L, JFE Advantech, Nishinomiya, Japan) during the experiments.

The assessment of the biomass and species composition was conducted in March 2019. Two transect lines were set from the shoreline to the edge of the macroalgal bed to document the biomass, coverage, and species composition of the macroalgae (Fig. 1). To assess the coverage and species composition, 1 m × 1 m quadrats were located at 10-m intervals along each transect. SCUBA divers quantified the apparent vegetation coverage and species composition in each quadrat. Five quadrats (0.5 m × 0.5 m) were located in the area dominated by sargassaceous algae along each transect to quantify the biomass of algae. SCUBA divers collected all macroalgae in each quadrat. The wet weight of the sargassaceous algae and the other macroalgae were then measured immediately.

2.2 Degradation experiment

DOC samples for degradation experiments were obtained after the field bag experiments. Water samples were collected from each transparent bag of macroalgae and ambient seawater. The samples were filtered through precombusted (450 °C for 2 h) glass fibre filters (GF/F, Whatman, Maidstone, Kent, UK). We assumed that GF/F filters would allow the passage of a significant fraction of free-living bacteria into the experimental samples (e.g., Wada et al., 2008; Bauer and Bianchi, 2011; Kubo et al., 2015).

The filtrates were transferred into precombusted (450 °C for 2 h) 100-ml glass vials sealed with rubber and aluminium caps. The degradation experiments were conducted based on a total of six incubations (0, 3, 10, 30, 90, and 150 days) per field survey. Triplicate bottles were used for each incubation. The experimental samples were stored at room temperature (22 °C) in total darkness until analysis. After incubation, the samples were filtered through 0.2-µm polytetrafluoroethylene filters (DISMIC–25HP; Advantec, Durham, NC, USA) into precombusted (450 °C for 2 h) 100-ml glass vials and frozen at −20 °C until analysis.

In this study, the concentration of refractory DOC (RDOC) was defined as the concentration of DOC remaining after 150 days, and the concentration of DOC derived from macroalgae (DOC_M) was equated to the difference between the DOC concentration in the macroalgae bag and the DOC concentration in the control bag (DOC_C).

2.3 Sample analyses

The DIC concentration and TAlk were determined with a batch-sample analyser (ATT-05 and ATT-15; Kimoto Electric, Osaka, Japan) according to Tokoro et al. (2014). The analytical precision of the system, based on the standard deviation of multiple reference replicates, was normally within ±2 µmol L^{-1} for DIC and TAlk.

DOC concentrations were measured at least in triplicate with a total organic carbon analyser (TOC-L; Shimadzu, Kyoto, Japan) according to Ogawa et al. (1999). Potassium hydrogen phthalate (Wako Pure Industries, Osaka, Japan) was used as a standard for the measurement. The coefficient of variation of the analyses was less than 2 %.

https://doi.org/10.5194/bg-2019-448
Preprint. Discussion started: 19 November 2019

2.4 Air–water CO_2 flux

The air–water CO_2 flux (FCO_2) was determined by using the bulk formula method. The equation for the method is as follows:

$$FCO_2 = -KS\,(fCO_{2water} - fCO_{2air}) \quad (1)$$

The gas transfer velocity (K) in Eq. (1) was determined from empirical relationships between K and the wind speed above the surface of the water (e.g., Wanninkhof, 1992; McGillis et al., 2001). A positive FCO_2 value indicates CO_2 absorption from the air to the water. We here used the following empirical equation to estimate K (Wanninkhof, 1992):

$$K = 0.39 U_{10}^2\,(Sc / 660)^{-0.5}, \quad (2)$$

where U_{10} is the wind speed at a height of 10 m above the water surface. We determined U_{10} by assuming that there was a logarithmic relationship between wind speed, height, and the roughness of the water surface (Kondo, 2000). Wind speed was obtained from Automated Meteorological Data Acquisition System (AMeDAS) data provided by the Japan Meteorological Agency and was measured about 10 km away at Agenosho. The Schmidt number (Sc) was determined from the water temperature and salinity of the water surface.

The solubility (S) of CO_2 is a function of water temperature and salinity (Weiss, 1974). fCO_{2water} and fCO_{2air} are the fugacity of CO_2 in water and that in air, respectively. fCO_{2water} was estimated by using chemical equilibrium relationships and the TAlk and DIC of the water samples (Zeebe and Wolf-Gladrow, 2001). The average salinity and water temperature were used to calculate fCO_{2water} in each survey. We used the averaged fCO_{2air} (410 µatm) measured with a CO_2 analyser (CO2-09; Kimoto Electric, Osaka, Japan).

2.5 Mass balance modelling

The diurnal changes and budgets of the carbonate system and DOC were simulated by mass balance models of the macroalgal bed. The mass balance models of the macroalgal bed simulated a hypothetical average macroalgal bed covering an area of 1 m^2. The average depth of the hypothetical macroalgal bed was the same as that of the macroalgal bed at the study site (2.0 m), and the depth was changed to simulate the actual tide. We used the average biomass of sargassaceous algae in the mass balance models.

Time course changes in the concentrations of DIC, TAlk, and DOC (µmol L^{-1}) in the macroalgal bed were calculated at hourly time intervals. The duration of the simulation was 24 h beginning at sunrise of the survey day. The initial values in the simulation were defined as the average values at the offshore site (station H5). Each concentration at time step (t) was calculated from the concentration at time step (t−1) as follows:

$$DIC_t = (DIC_{t-1} - GCP + R - CC + FCO_2) \times (1 - EX) + DIC_O \times EX \quad (3)$$

https://doi.org/10.5194/bg-2019-448
Preprint. Discussion started: 19 November 2019

$$TAlk_t = (TAlk_{t-1} - 2CC) \times (1 - EX) + TAlk_O \times EX \quad (4)$$

$$DOC_t = (DOC_{t-1} + NDR) \times (1 - EX) + DOC_O \times EX \quad (5)$$

Gross community production (GCP; μmol L^{-1} h^{-1}), community respiration (R; μmol L^{-1} h^{-1}), community calcification (CC; μmol L^{-1} h^{-1}), and net DOC release (NDR; μmol L^{-1} h^{-1}) were determined from the results of the field bag experiments (Table S1 in the Supplement). These metabolic parameters were calculated as the sum of the contributions from both macroalgae and phytoplankton. The values of DIC_O, $TAlk_O$, and DOC_O were the mean values at station H5. We assumed that there was no biogeochemical exchange between the bottom substrate and water. In the simulation, the metabolic parameters (GCP, R, CC, and NDR) of *S. horneri* were assumed to apply to the entire macroalgal bed. We used different metabolic parameters during the day and night. EX ($0 \leq EX \leq 1$), the hourly water exchange rate, was defined as follows:

$$EX = EX_{tide} + EX_r, \quad (6)$$

where EX_{tide} indicates the water exchange rate due to tidal change. EX_{tide} was estimated from the changes of depth, and was positive during the flood tide and zero during the ebb tide. EX_r was defined as the residual exchange rate due to factors other than tidal change. EX_r was determined by fitting the DIC model so as to minimize the root mean squared error (RMSE) compared with the observed DIC values because the observed DIC values were the most variable in the concentrations in this study and were suitable for such model fitting. This model fitting was performed using the daytime data. The estimated EX_r was applied throughout the diurnal cycle on the assumption that EX_r was comparable during the day and night. The budgets of DIC, TAlk, and DOC were calculated as the net gain or loss of each constituent due to water exchange. The changes in fCO_2, which were estimated using chemical equilibrium relationships and the TAlk and DIC of the water samples (Zeebe and Wolf-Gladrow, 2001), were used to calculate FCO_2. The average salinity and water temperature were used to calculate fCO_2 in each survey.

2.6 Statistical analyses

Statistical analyses were performed by using the R statistical packages (R Core Team, 2019). We used a Welch's two-sample *t*-test to determine whether there were differences in salinity, DIC, TAlk, fCO_2, and DOC between the macroalgal bed and the offshore site.

3 Results

3.1 Carbonate system and DOC in the macroalgal bed

There were no differences in salinity and TAlk between the macroalgal bed (n = 12) and the offshore site (n = 3) (Welch's two-sample *t*-test, $p > 0.05$; Table 1) in both February and March. The DIC concentration was significantly lower in the

https://doi.org/10.5194/bg-2019-448
Preprint. Discussion started: 19 November 2019

macroalgal bed (1964 ± 22 μmol L^{-1}) than at the offshore site (1991 ± 1 μmol L^{-1}) in February (p = 0.002). In March, the variation of the DIC concentration was large (1962 ± 43 μmol L^{-1}) in the macroalgal bed but was also significantly lower than at the offshore site (1992 ± 1 μmol L^{-1}) (p = 0.033). The fCO_2 values were significantly lower in the macroalgal bed than at the offshore site in both February (p = 0.001) and March (p = 0.025). The fCO_2 values in the macroalgal bed (February, 265 ± 31 μatm; March, 272 ± 49 μatm) and the offshore site (February, 305 ± 3 μatm; March, 309 ± 1 μatm) were lower than fCO_{2air} (410 μatm). The DOC concentration was significantly higher in the macroalgal bed than at the offshore site during March (p = 0.010). The DOC concentration was slightly higher in the macroalgal bed than at the offshore site during February, but there was no significant difference between the two (p > 0.05). fCO_2 was strongly correlated with DIC in both February and March (Fig. 2). The homogeneous buffer factors (β), which were obtained as the slopes of log-log plots of fCO_2 versus DIC, were 10.81 and 9.36 in February and March, respectively.

Community carbon metabolism was calculated from the field-bag experiments (Table 2 and Table S3 in the Supplement). The net community production (NCP) of macroalgae was about four times higher in March (1390 mmol-C m^{-2} d^{-1}) than in February (314 mmol-C m^{-2} d^{-1}) (Table 2). The NCP of macroalgae was considerably higher than that of phytoplankton (~13 mmol-C m^{-2} d^{-1}). The net community calcification (NCC) of macroalgae was positive (~21 mmol-C m^{-2} d^{-1}), but the values were much lower than the NCP values. The net DOC release of macroalgae was 107 mmol-C m^{-2} d^{-1} and 88 mmol-C m^{-2} d^{-1} in February and March, respectively. These values were equivalent to about 34 % and 6 % of the NCP in February and March, respectively.

3.2 Biomass and species composition of macroalgae

The macroalgal bed was dominated by sargassaceous algae (Fig. 3 and Figs. S1 and S2 in the Supplement). The biomass of sargassaceous algae (mean: 4693 g-ww m^{-2}) was higher than that of the other macroalgae (264 g-ww m^{-2}) (Fig. 3). The coverage of sargassaceous algae (~80 %) was also larger than that of the other macroalgae (~51 %).

3.3 Degradation of DOC

DOC concentrations collected from macroalgae bags decreased with time in both experiments (Fig. 4). In contrast, DOC concentrations collected from control bags were stable during the experiments. DOC_M gradually decreased with time. Refractory DOC_M ($RDOC_M$) concentrations were 56 ± 4 % and 78 ± 27 % of initial DOC_M concentrations in February and March, respectively (Fig. 4c). Degradation rates (k) estimated by exponential fitting were 0.0044 d^{-1} and 0.0018 d^{-1} in February and March, respectively.

3.4 Carbon budgets estimated using mass balance models

The mass balance models simulated the temporal changes in carbonate chemistry and DOC concentration (Fig. 5). The EX_r values were 35 % and 50 % in February and March, respectively (Table 3). The RMSEs for DIC model fitting were 9 μM

https://doi.org/10.5194/bg-2019-448
Preprint. Discussion started: 19 November 2019

and 25 µM, respectively. Hourly water exchange rates (*EX*s) were estimated to be 35–48 % and 50–76 % in February and March, respectively (Table 3).

The models were improved by considering water exchange (Fig. 5). DIC concentrations were decreased in the daytime by primary production (Fig. 5a, e). TAlk values in the macroalgal bed were stable and very similar to the TAlk values of the offshore seawater (Fig. 5b, f). The fCO_2 decreased during the daytime because of the concurrent decrease of the DIC concentration (Fig. 5c, g). DOC concentrations in the macroalgal bed exceeded those at the offshore site during the daytime (Fig. 5d, h).

DIC budgets driven by water exchange indicated a net input of DIC from offshore to the macroalgal bed (Fig. 6 and Table 3). The areal influxes of DIC were 337 mmol-C m^{-2} d^{-1} and 1393 mmol-C m^{-2} d^{-1} in February and March, respectively. These fluxes were almost equivalent to the sum of NCP, NCC, and FCO_2 in the macroalgal bed (Fig. 6). DOC was exported from the macroalgal bed to offshore. The areal effluxes of DOC (February: 124 mmol-C m^{-2} d^{-1}, March: 97 mmol-C m^{-2} d^{-1}) were similar to the NDRs. The export fluxes of $RDOC_M$ were estimated to be 58 mmol-C m^{-2} d^{-1} and 67 mmol-C m^{-2} d^{-1} in February and March, respectively. The FCO_2 values showed that both the macroalgal bed and the offshore site absorbed atmospheric CO_2 during these study periods. FCO_2 values were higher in the macroalgal bed than offshore during both periods.

4 Discussion

4.1 CO_2 absorption and DIC budgets in macroalgal bed

Atmospheric CO_2 absorption was affected by community metabolism and water exchange, which regulated the carbon budget in the sargassaceous algae–dominated macroalgal bed. Positive NCP values showed that the macroalgal bed acted as an autotrophic system during the study periods. Macroalgal DIC uptake (i.e., NCP) accounted for >97 % of total NCP in this system (Table 2). Biological uptake of DIC promoted atmospheric CO_2 absorption by contributing to the decrease of DIC concentrations and fCO_2 during the day inside the macroalgal bed (Figs. 5 and 6).

Previous studies have shown that macroalgal primary production reduces DIC and CO_2 concentrations. DIC uptake by kelp reduces fCO_2 and thereby contributes to the absorption of atmospheric CO_2 inside kelp beds (Delille et al., 2000, 2009; Koweek et al., 2017; Pfister et al., 2019). The aquaculture of macroalgal species such as the kelp *Laminaria japonica* and the red alga *Gracilaria lemaneiformis* has also been known to result in annual net uptake of CO_2 because of active photosynthesis by the macroalgae (Jiang et al., 2013). In contrast, knowledge about in situ carbonate chemistry in beds of sargassaceous algae is limited (e.g., Tokoro et al., 2019). The present study, however, has shown that a bed of sargassaceous algae takes up atmospheric CO_2 over a diurnal cycle during productive periods of the year.

Our results show that metabolism and water exchange regulated the diurnal variations in DIC and fCO_2 in the macroalgal bed. Our mass balance model analyses suggest that the high rate of water inflow from the outside of the bed strongly affected DIC concentrations and fCO_2 in the macroalgal bed (Fig. 5a, e). The decrease of the DIC concentration of the macroalgal

https://doi.org/10.5194/bg-2019-448
Preprint. Discussion started: 19 November 2019

bed was moderated by water exchange during the day. The high rate of water exchange reduced the difference in FCO_2 between the inside and outside of the macroalgal beds (Fig. 6). Conversely, water characterized by low DIC and fCO_2 values was efficiently exported from the macroalgal bed to the surrounding water (Fig. 6). Our findings therefore suggest that macroalgal beds create areas of adjacent water that serve as CO_2 sinks. Previous studies have proposed that a canopy of the kelp genus *Macrocystis* dampens water exchange (Rosman et al., 2007), and the residence time of water within kelp beds can reach several days (Jackson and Winant, 1983; Delille et al., 2009). In contrast, the exposed side of a kelp bed is very much affected by the advection of offshore water (Koweek et al., 2017). Water exchange rates are affected by the surface area of beds, canopy development, topography, and hydrological conditions.

The seasonality of the growth of macroalgae regulates the seasonal variations of carbonate chemistry and sink/source behaviour (Delille et al., 2009; Koweek et al., 2017). Annual fluctuations of the surface area of kelp beds affect interannual variations in air–sea CO_2 fluxes in adjacent water bodies (Ikawa and Oechel, 2015). In the present study, we focused on how daily carbon budgets were related to macroalgal metabolism and hydrological conditions during productive periods. The biomass of sargassaceous algae fluctuates seasonally and increases in winter (from November to April) around the present study site (Yoshida et al., 2001). Future studies should assess the seasonal variability of carbonate chemistry in sargassaceous algal beds.

The homogenous buffer factor (β) is a general and helpful tool that can be used to identify the main processes that affect carbonate chemistry dynamics (e.g., Frankignoulle, 1994). Frankignoulle (1994) found the relationship $\beta = -7.02 + 0.186 \times \%C_{org}$, where $\%C_{org}$ is the percent change of the DIC concentrations due to photosynthesis and respiration. By using this equation, we calculated the $\%C_{org}$ to be 96 % and 88 % in February and March, respectively (Fig. 2). The results therefore indicate that NCP was the main regulator of carbonate chemistry, and the contribution of NCC was relatively small. This conclusion is consistent with the results of the field bag experiments (Table 2).

4.2 Community metabolism in the macroalgal bed

Macroalgal NCP values in the present study (314–1390 mmol-C m^{-2} d^{-1}) are comparable to those in a sub-Arctic kelp bed (~1250 mmol-C m^{-2} d^{-1}; Delille et al., 2009) and to gross primary production in a *Macrocystis* kelp bed in California (~570 mmol-C m^{-2} d^{-1}; Towle and Pearse, 1973; Jackson, 1987) and in an *Ecklonia* kelp bed (464 mmol-O_2 m^{-2} d^{-1}; Randall et al., 2019); they are much larger than the NCP values in a calcareous macrophyte bed (19 mmol-C m^{-2} d^{-1}; Bensoussan and Gattuso, 2007) and on a coral reef dominated by green and red algae (−112 to 61 mmol-C m^{-2} d^{-1}; Falter et al., 2001). The inhibition of macroalgal R by low water temperatures during the winter can explain the relatively high NCP values during the productive period at our study site (Table 1 and 2). The macroalgal NCP value during March was four times higher than the value during February in the present study (Table 2). Irradiation, day length, and growth phase collectively control the temporal variations of macroalgal NCP.

The relative growth rates (% d^{-1}) of *S. horneri* were calculated to be 1.2–7.4 % d^{-1} based on the ratio of growth (= NCP − NDR) to biomass (Table S1 in the Supplement). To calculate biomass, we assumed that the water content was 85 % of wet

https://doi.org/10.5194/bg-2019-448
Preprint. Discussion started: 19 November 2019

weight and that carbon content was 30 % of dry weight (Watanabe et al., unpublished data). These relative growth rates are comparable to estimates based on biomass changes of *S. horneri* (around 4 % d^{-1}, Gao and Hua, 1997; Choi et al., 2008) and *S. muticum* (~10 % d^{-1}, Pedersen et al., 2005). The estimated uncertainties of NCP and NCC derived from the measurement precision of DIC and TAlk were ~26 mmol-C m^{-2} d^{-1} and ~13 mmol-C m^{-2} d^{-1}, respectively. Hence, it is difficult to discuss NCC values and phytoplankton NCP values (Table 2), but these values were substantially lower than macroalgal NCP values in this study.

4.3 Refractory DOC release by macroalgae

Our results showed that the sargassaceous algal bed released a large amount of DOC (Fig. 6). Most of the released DOC was exported out of the macroalgal bed via water exchange during the day. The DOC release rates of *S. horneri* (18.7–22.8 μmol-C g-ww^{-1} d^{-1}, Table S1 in the Supplement) are within the range of those reported for *Ecklonia* kelp (1.5–72.5 μmol-C g-ww^{-1} d^{-1}, Wada et al., 2007), which were converted by assuming that water content was 85 % of wet weight (Watanabe et al., unpublished data). The fact that Wada et al. (2007) collected data over an entire year whereas our data were collected during only the most productive two months of the year accounts for the difference in the variations of DOC release rates. Previous studies have found that a substantial portion of production is released as DOC by kelps (18–62 %, Abdullah and Fredriksen, 2004; Wada et al., 2007). Our results showed that sargassaceous algae sometimes release a similar percentage of production as DOC, but the percentages were very different between February (34 %) and March (6 %) (Fig. 6). DOC release by kelps has been shown to be correlated with irradiation, but irradiation explained only 13 % of the variation of the DOC release rates (Reed et al., 2015). Time lags between light-stimulated carbon assimilation and DOC release may explain some of the variation between irradiance and DOC release. High-frequency time-series measurements may help to explain the daily variations of macroalgal carbon metabolism.

Refractory organic carbon acts as a carbon reservoir in seawater (Hansell and Carlson, 2015) and is considered to be one of the important contributors to carbon sequestration by coastal macrophytes (Maher and Eyre, 2010; Watanabe and Kuwae, 2015; Krause-Jensen and Duarte, 2016; Duarte and Krause-Jensen, 2017). Wada et al. (2008) have estimated the turnover times of the DOC released by *Ecklonia* kelp, the reciprocals of the degradation rates (k), to be 24–172 days (k values, 0.0058–0.0407 d^{-1}). In the present study, the turnover times of DOC released by *S. horneri* were calculated to be 227–556 days (k values, 0.0018–0.0044 d^{-1}), longer than the turnover times of *Ecklonia* kelp. These findings indicate that the recalcitrance of macroalgal DOC is variable and depends on the species and environmental conditions.

The fact that the turnover times of macroalgal DOC are longer than those of DOC released by phytoplankton (~40 days; Hama et al., 2004; Kirchman et al., 1991) implies that macroalgal DOC is more biologically recalcitrant than DOC produced by phytoplankton (Wada et al., 2008). Previous studies have suggested that macroalgae produce phenolic compounds, which are biologically recalcitrant (Swanson and Druehl, 2002; Wada and Hama, 2013; Powers et al., 2019). A thermogravimetric approach has also shown that macroalgal thalli contain refractory compounds (Trevathan-Tackett et al., 2015), some of

https://doi.org/10.5194/bg-2019-448
Preprint. Discussion started: 19 November 2019

313 which are released as the plant grows. These findings indicate that macroalgae release chemically recalcitrant DOC for
314 decomposers.
315 Ogawa et al. (2001) have shown that marine bacteria take up labile organic matter (OM) such as glucose and convert it
316 into refractory OM. Some of the macroalgal DOC may be converted to refractory OC by microbes and persist in water for a
317 long time. Carbon flows through the microbial loop should be assessed as one of the fates of OM derived from macroalgal
318 beds.

319 **4.4 Implications for the CO_2 sequestration function of macroalgae**

320 Macroalgal beds are potential carbon-donor sites in the context of Blue Carbon functions (Krause-Jensen et al., 2018). The
321 export of macroalgal thalli and fragments to the deep sea via physical processes would contribute to CO_2 sequestration
322 (Krause-Jensen and Duarte 2016). The export of recalcitrant DOC from macroalgal beds is also anticipated to be an
323 important pathway for CO_2 sequestration (Wada and Hama, 2013; Barrón et al., 2014; Reed et al., 2015). Our results show
324 that a sargassaceous algal bed released substantial amount of RDOC, which was rapidly exported from the habitat to the
325 offshore. The residence time of ~200 days of dissolved matter in the western Seto Inland Sea (Balotro et al., 2002) indicates
326 that macroalgal DOC can be exported to the outside of the inland sea and reach the deep sea via vertical mixing.
327 The decrease in fCO_2 due to macroalgal DIC uptake directly controls the influx of atmospheric CO_2 into macroalgal
328 habitats and the waters surrounding them. The present study showed that the metabolism of sargassaceous algae mediated
329 the production of low-DIC and low-fCO_2 water, which was rapidly exported to outside of the habitat. Because macroalgae
330 commonly inhabit rocky reefs facing the open ocean, macroalgal metabolism may affect a wide range of water bodies
331 surrounding rocky reef habitats (e.g., Ikawa and Oechel, 2015). The CO_2 sequestration function of macroalgae found in
332 habitats where macroalgae-affected water easily diffuses offshore has been overlooked.
333 Studies of the role of macroalgae in CO_2 sequestration should use field observations and coupled ecological-physical
334 models to assess the spatial spread and fate of DOC and low-fCO_2 waters derived from macroalgal habitats (Kuwae et al.,
335 2019; Macreadie et al., 2019). Such studies will lead to a better understanding of the role of macroalgae in sequestering Blue
336 Carbon and thereby mitigating global climate change.

337 **5 Conclusions**

338 The present study showed that macroalgal metabolism and lateral carbon flows regulated carbon budgets and air–water CO_2
339 exchange in a temperate macroalgal bed and its surrounding water. Macroalgae absorbed DIC via photosynthesis and
340 released large amounts of DOC to the offshore waters adjacent to the bed. Hydrological water exchange enhanced the lateral
341 carbon flows and the spread to the surrounding water of low-fCO_2 and high-DOC water mediated by macroalgal metabolism.
342 Our findings suggest that macroalgal beds create areas of adjacent water that serve as CO_2 sinks. These results suggest the
343 need for future research to assess the areal extent and fate of macroalgae-mediated low-fCO_2 and high-DOC waters.

https://doi.org/10.5194/bg-2019-448
Preprint. Discussion started: 19 November 2019

Data availability

Research data can be accessed by contacting the authors.

Author contributions

KW, GY, MH, YU and TK conceived the study. KW, GY, MH, HM and TK collected the samples. KW and HM conducted the laboratory analyses. KW and TK processed the data. KW and TK wrote the paper with substantial input from the other authors.

Competing interests

The authors declare that they have no conflict of interest.

Acknowledgements. This study was funded in part by KAKENHI grant numbers JP18H04156, 19K20500, and 19K12295 from the Japan Society for the Promotion of Science. We thank A. Kajita and K. Manabe for help in field observations and N. Umegaki, H. Shimada, and R. Makino for chemical analyses.

References

Abdullah, M.I. and Fredriksen, S.: Production, respiration and exudation of dissolved organic matter by the kelp *Laminaria hyperborea* along the west coast of Norway, J. Mar. Biol. Assoc. U. K., 84, 887–894, https://doi.org/10.1017/S002531540401015Xh, 2004.

Balotro, R. S., Isobe, A., Shimizu, M., Kaneda, A., Takeuchi, T., and Takeoka, H.: Circulation and Material Transport in Suo-Nada during Spring and Summer, J. Oceanogr., 58, 759–773, https://doi.org/10.1023/A:1022858710221, 2002.

Barrón, C., Apostolaki, E. T., and Duarte, C. M.: Dissolved organic carbon fluxes by seagrass meadows and macroalgal beds, Front. Mar. Sci., 1, 42, https://doi.org/10.3389/fmars.2014.00042, 2014.

Bauer, J. E. and Bianchi, T. S.: Dissolved Organic Carbon Cycling and Transformation, in: Treatise on Estuarine and Coastal Science, edited by: Wolanski, E. and McLusky, D. S., Academic Press, Sam Diego, CA, USA, 7–67, https://doi.org/10.1016/B978-0-12-374711-2.00502-7, 2011.

Bauer, J. E. and Druffel, E. R.: Ocean margins as a significant source of organic matter to the deep open ocean, Nature, 92, 482–485, https://doi.org/10.1038/33122, 1998.

Bensoussan, N. and Gattuso, J.-P.: Community primary production and calcification in a NW Mediterranean ecosystem dominated by calcareous macroalgae, Mar. Ecol. Progr. Ser., 334, 37–45, https://doi.org/10.3354/meps334037, 2007.

370 Choi, H. G., Lee, K. H., Yoo, H. I., Kang, P. J., Kim, Y. S., and Nam, K. W.: Physiological differences in the growth of
371 *Sargassum horneri* between the germling and adult stages, J. Appl. Phycol., 20, 729–35, https://doi.org/10.1007/s10811-
372 007-9281-5, 2008.
373 Delille, B., Borges A. V., and Delille, D.: Influence of giant kelp beds (*Macrocystis pyrifera*) on diel cycles of pCO_2 and
374 DIC in the Sub-Antarctic coastal area, Estuar. Coast. Shelf Sci., 81, 114–122, https://doi.org/10.1016/j.ecss.2008.10.004,
375 2009.
376 Delille, B., Dellile, D., Fiala, M., Prevost, C., and Frankignoulle. M.: Seasonal changes of pCO_2 over a subantarctic
377 *Macrocystis* kelp bed, Polar Biol., 23, 706–716, https://doi.org/10.1007/s003000000142, 2000.
378 Duarte, C. M.: Submerged aquatic vegetation in relation to different nutrient regimes, Ophelia, 41, 87–112,
379 https://doi.org/10.1080/00785236.1995.10422039, 1995.
380 Duarte, C. M.: Reviews and syntheses: Hidden forests, the role of vegetated coastal habitats in the ocean carbon budget,
381 Biogeosciences, 14, 301–310, https://doi.org/10.5194/bg-14-301-2017, 2017.
382 Duarte, C. M. and Krause-Jensen, D.: Export from Seagrass Meadows Contributes to Marine Carbon Sequestration, Front.
383 Mar. Sci., 4, 13, https://doi.org/10.3389/fmars.2017.00013, 2017.
384 Duarte, C. M., Losada, I. J., Hendriks, I. E., Mazarrasa, I., and Marbà, N.: The role of coastal plant communities for climate
385 change mitigation and adaptation, Nat. Clim. Change, 3, 961–968, https://doi.org/10.1038/nclimate1970, 2013.
386 Falter, J. L., Atkinson, M. J., and Langdon, C.: Production–respiration relationships at different timescales within the
387 Biosphere 2 coral reef biome, Limnol. Oceanogr., 46, 1653–1660, https://doi.org/10.4319/lo.2001.46.7.1653, 2001.
388 Frankignoulle, M.: A complete set of buffer factors for acid/base CO_2 system in seawater, J. Mar. Syst., 5, 111–118,
389 https://doi.org/10.1016/0924-7963(94)90026-4, 1994.
390 Gao, K. and Hua, W.: *In situ* growth rates of *Sargassum horneri* (Fucales, Phaeophyta), Phycol. Res., 45, 55–57,
391 https://doi.org/10.1111/j.1440-1835.1997.tb00062.x, 1997.
392 Hama, T., Yanagi, K., and Hama, J.: Decrease in molecular weight of photosynthetic products of marine phytoplankton
393 during early diagenesis, Limnol. Oceanogr., 49, 471–481, https://doi.org/10.4319/lo.2004.49.2.0471, 2004.
394 Hansell, D. A. and Carlson, C. A. (Eds.): Biogeochemistry of Marine Dissolved Organic Matter, Academic Press, San Diego,
395 CA, USA, https://doi.org/10.1016/C2012-0-02714-7, 2015.
396 Ikawa, H. and Oechel, W. C.: Temporal variations in air-sea CO_2 exchange near large kelp beds near San Diego, California,
397 J. Geophys. Res. Oceans, 120, 50–63, https://doi.org/10.1002/2014JC010229, 2015.
398 Jackson, G.A.: Modelling the growth and harvest yield of the giant kelp *Macrocystis pyrifera*, Mar. Biol., 95, 611–624,
399 https://doi.org/10.1007/BF00393105, 1987.
400 Jackson, G.A. and Winant, C.D.: Effect of a kelp forest on coastal currents, Continent. Shelf Res., 2, 75–80,
401 https://doi.org/10.1016/0278-4343(83)90023-7, 1983.
402 Jiang, Z., Fang, J., Mao, Y., Han, T., and Wang, G.: Influence of Seaweed Aquaculture on Marine Inorganic Carbon
403 Dynamics and Sea-air CO_2 Flux, J. World Aquaculture Soc., 44, 133–140, https://doi.org/10.1111/jwas.12000, 2013.

404 Kirchman, D. L., Suzuki, Y., Garside, C., and Ducklow, H. W.: High turnover rates of dissolved organic carbon during a
405 spring phytoplankton bloom, Nature, 352, 612–614, https://doi.org/10.1038/352612a0, 1991.
406 Kondo, J.: Atmosphere Science near the Ground Surface, University of Tokyo Press, Tokyo, Japan, 2000.
407 Koweek, D. A., Nickols, K. J., Leary, P. R., Litvin, S. Y., Bell, T. W., Luthin, T., Lummis, S., Mucciarone, D. A., and
408 Dunbar, R. B.: A year in the life of a central California kelp forest: physical and biological insights into biogeochemical
409 variability, Biogeosciences, 14, 31–44, https://doi.org/10.5194/bg-14-31-2017, 2017.
410 Krause-Jensen, D. and Duarte, C. M.: Substantial role of macroalgae in marine carbon sequestration, Nat. Geosci., 9, 737–
411 742, https://doi.org/10.1038/ngeo2790, 2016.
412 Krause-Jensen, D., Lavery, P., Serrano, O., Marbà, N., Masque, P., and Duarte, C. M.: Sequestration of macroalgal carbon:
413 the elephant in the Blue Carbon room, Biol. Lett., 14, 20180236, http://dx.doi.org/10.1098/rsbl.2018.0236, 2018.
414 Kubo, A, Yamamoto-Kawai, M, and Kanda, J.: Seasonal variations in concentration and lability of dissolved organic carbon
415 in Tokyo Bay, Biogeosciences, 12, 239–279, https://doi.org/10.5194/bg-12-269-2015, 2015.
416 Kuwae, T., Kanda, J., Kubo, A., Nakajima, F., Ogawa, H., Sohma, A., and Suzumura, M.: CO_2 Uptake in the Shallow
417 Coastal Ecosystems Affected by Anthropogenic Impacts, in: Blue Carbon in Shallow Coastal Ecosystems: Carbon
418 Dynamics, Policy, and Implementation, edited by: Kuwae, T. and Hori, M., Springer, Singapore, 295–319,
419 https://doi.org/10.1007/978-981-13-1295-3_11, 2019.
420 Macreadie, P. I., Anton, A., Raven, J. A., Beaumont, N., Connolly, R. M., Friess, D. A., Kelleway, J. J., Kennedy, H.,
421 Kuwae, T., Lavery, P. S., Lovelock, C. E., Smale, D. A., Apostolaki, E. T., Atwood, T. B., Baldock, J., Bianchi, T. S.,
422 Chmura, G. L., Eyre, B. D., Fourqurean, J. W., Hall-Spencer, J. M., Huxham, M., Hendriks, I. E., Krause-Jensen, D.,
423 Laffoley, D., Luisetti, T., Marbà, N., Masque, P., McGlathery, K. J., Megonigal, J. P., Murdiyarso, D., Russell, B. D.,
424 Santos, R., Serrano, O., Silliman, B. R., Watanabe, K., and Duarte, C. M.: The future of Blue Carbon science, Nat. Comm.,
425 10, 3998, https://doi.org/10.1038/s41467-019-11693-w, 2019.
426 Maher, D. T. and Eyre, B. D.: Benthic fluxes of dissolved organic carbon in three temperate Australian estuaries:
427 Implications for global estimates of benthic DOC fluxes, J. Geophys. Res. Biogeosci., 115, G04039,
428 https://doi.org/10.1029/2010JG001433, 2010.
429 McGillis, W. R., Edson, J. B., Ware, J. D., Dacey, J. W. H., Hare, J. E., Fairall, C. W., and Wanninkhof, R.: Carbon dioxide
430 flux techniques performed during GasEx-98., Mar. Chem., 75, 267–280, https://doi.org/10.1016/S0304-4203(01)00042-1,
431 2001.
432 Mcleod, E., Chmura, G. L., Bouillon, S., Salm, R., Björk, M., Duarte, C. M., Lovelock, C. E., Schlesinger, W. H., and
433 Silliman, B. R.: A blueprint for blue carbon: toward an improved understanding of the role of vegetated coastal habitats in
434 sequestering CO_2, Front. Ecol. Environ., 9, 552–560, https://doi.org/10.1890/110004, 2011.
435 Miyajima T. and Hamaguchi M.: Carbon Sequestration in Sediment as an Ecosystem Function of Seagrass Meadows, in:
436 Blue Carbon in Shallow Coastal Ecosystems: Carbon Dynamics, Policy, and Implementation, edited by: Kuwae, T. and
437 Hori, M., Springer, Singapore, 33–71, https://doi.org/10.1007/978-981-13-1295-3_2, 2019.

https://doi.org/10.5194/bg-2019-448
Preprint. Discussion started: 19 November 2019

438 Nellemann, C., Corcoran, E., Duarte, C. M., Valdés, L., De Young, C., Fonseca, L., and Grimsditch, G.: Blue carbon. A
439 rapid response assessment, United Nations Environmental Programme, Arendal, Norway, 2009.
440 Ogawa, H., Amagai, Y., Koike, I., Kaiser, K., and Benner, R.: Production of Refractory Dissolved Organic Matter by
441 Bacteria, Science, 292, 917–920, https://doi.org/10.1126/science.1057627, 2001.
442 Ogawa, H., Fukuda, R., and Koike, I.: Vertical distributions of dissolved organic carbon and nitrogen in the Southern Ocean,
443 Deep Sea Res. I, 46, 1809–1826, https://doi.org/10.1016/S0967-0637(99)00027-8, 1999.
444 Pedersen, M. F., Stæhr, P. A., Wernberg, T., and Thomsen, M. S.: Biomass dynamics of exotic *Sargassum muticum* and
445 native *Halidrys siliquosa* in Limfjorden, Denmark—Implications of species replacements on turnover rates, Aquat. Bot.,
446 83, 31–47, https://doi.org/10.1016/j.aquabot.2005.05.004, 2005.
447 Pfister, C. A., Altabet, M. A., and Weigel, B. L.: Kelp beds and their local effects on seawater chemistry, productivity, and
448 microbial communities, Ecology, 100, e02798, https://doi.org/10.1002/ecy.2798, 2019.
449 Powers, L. C., Hertkorn, N., McDonald, N., Schmitt-Kopplin, P., Del Vecchio, R., Blough, N. V., and Gonsior, M.:
450 *Sargassum* sp. act as a Large Regional Source of Marine Dissolved Organic Carbon and Polyphenols, Global Biogeochem.
451 Cy., https://doi.org/10.1029/2019GB006225, 2019.
452 Randall, J., Wotherspoon, S., Ross, J., Hermand, J. P., and Johnson, C. R.: An *in situ* study of production from diel oxygen
453 modelling, oxygen exchange, and electron transport rate in the kelp *Ecklonia radiate*, Mar. Ecol. Prog. Ser., 615, 51-65,
454 https://doi.org/10.3354/meps12919, 2019.
455 Raven, J.: Blue carbon: past, present and future, with emphasis on macroalgae, Biol. Lett., 14, 20180336,
456 http://dx.doi.org/10.1098/rsbl.2018.03363, 2018.
457 R Core Team: R: A language and environment for statistical computing, R Foundation for Statistical Computing, Vienna,
458 Austria, https://www.R-project.org/, 2019.
459 Reed, D. C., Carlson, C. A., Halewood, E. R., Nelson, J. C., Harrer, S. L., Rassweiler, A., and Miller, R. J.: Patterns and
460 controls of reef-scale production of dissolved organic carbon by giant kelp *Macrocystis pyrifera*, Limnol. Oceanogr., 60,
461 1996–2008, https://doi.org/10.1002/lno.10154, 2015.
462 Rosman, J. H., Koseff, J. R., Monismith, S. G., and Grover, J.: A field investigation into the effects of a kelp forest
463 (*Macrocystis pyrifera*) on coastal hydrodynamics and transport, J. Geophys. Res. Oceans, 112, 1–16,
464 https://doi.org/10.1029/2005JC003430, 2007.
465 Swanson, A. K. and Druehl, L. D.: Induction, exudation and the UV protective role of kelp phlorotannins, Aquat. Bot., 73,
466 241–253, https://doi.org/10.1016/S0304-3770(02)00035-9, 2002.
467 Tokoro, T., Hosokawa, S., Miyoshi, E., Tada, K., Watanabe, K., Montani, S., Kayanne, H., and Kuwae, T.: Net uptake of
468 atmospheric CO_2 by coastal submerged aquatic vegetation, Global Change Biol., 20, 1873–1884,
469 https://doi.org/10.1111/gcb.12543, 2014.

https://doi.org/10.5194/bg-2019-448
Preprint. Discussion started: 19 November 2019

Tokoro, T., Watanabe, K., Tada, K., and Kuwae, T.: Air–Water CO_2 Flux in Shallow Coastal Waters: Theory, Methods, and Empirical Studies, in: Blue Carbon in Shallow Coastal Ecosystems: Carbon Dynamics, Policy, and Implementation, edited by: Kuwae, T. and Hori, M., Springer, Singapore, 153–184, https://doi.org/10.1007/978-981-13-1295-3_6, 2019.

Towle, D. W. and Pearse, J. S.: Production of the giant kelp, *Macrocystis*, by in situ incorporation of ^{14}C in polyethylene bags, Limnol. Oceanogr., 18, 155–159, https://doi.org/10.4319/lo.1973.18.1.0155, 1973.

Trevathan-Tackett, S. M., Kelleway, J., Macreadie, P. I., Beardall, J., Ralph, P., and Bellgrove, A.: Comparison of marine macrophytes for their contributions to blue carbon sequestration, Ecology, 96, 3043–3057, https://doi.org/10.1890/15-0149.1, 2015.

Wada, S., Aoki. M. N., Mikami, A., Komatsu, T., Tsuchiya, Y., Sato, T., Shinagawa, H., and Hama, T.: Bioavailability of macroalgal dissolved organic matter in seawater, Mar. Ecol. Prog. Ser., 370, 33-44, https://doi.org/10.3354/meps07645, 2008.

Wada, S., Aoki, M. N., Tsuchiya, Y., Sato, T., Shinagawa, H., and Hama, T.: Quantitative and qualitative analyses of dissolved organic matter released from *Ecklonia cava* Kjellman, in Oura Bay, Shimoda, Izu Peninsula, Japan, J. Exp. Mar. Biol. Ecol., 349, 344–358, https://doi.org/10.1016/j.jembe.2007.05.024, 2007.

Wada, S. and Hama, T.: The contribution of macroalgae to the coastal dissolved organic matter pool, Estuar. Coast. Shelf Sci., 129, 77–85, https://doi.org/10.1016/j.ecss.2013.06.007, 2013.

Wanninkhof, R.: Relationship between wind-speed and gas-exchange over the ocean, J. Geophys. Res. Oceans, 97, 7373–7382, https://doi.org/10.1029/92JC00188, 1992.

Watanabe, K. and Kuwae, T.: How organic carbon derived from multiple sources contributes to carbon sequestration processes in a shallow coastal system?, Global Change Biol., 21, 2612–2623, https://doi.org/10.1111/gcb.12924, 2015.

Weiss, R. F.: Carbon dioxide in water and seawater: the solubility of a non-ideal gas, Mar. Chem., 2, 203–215, https://doi.org/10.1016/0304-4203(74)90015-2, 1974.

Yoshida, G., Hori, M., Shimabukuro, H., Hamaoka, H., Onitsuka, T., Hasegawa, N., Muraoka, D., Yatsuya, K., Watanabe, K., and Nakaoka, M.: Carbon Sequestration by Seagrass and Macroalgae in Japan: Estimates and Future Needs, in: Blue Carbon in Shallow Coastal Ecosystems: Carbon Dynamics, Policy, and Implementation, edited by: Kuwae, T. and Hori, M., Springer, Singapore, 101–127, https://doi.org/10.1007/978-981-13-1295-3_4, 2019.

Yoshida, G., Yoshikawa, K., and Terawaki, T.: Growth and maturation of two populations of *Sargassum horneri* (Fucales, Phaeophyta) in Hiroshima Bay, the Seto Inland Sea, Fish. Sci., 67, 1023–1029, https://doi.org/10.1046/j.1444-2906.2001.00357.x, 2001.

Zeebe, R. E. and Wolf-Gladrow, D.: CO_2 in Seawater: Equilibrium, Kinetics, Isotopes, Elsevier, Amsterdam, Netherlands, 2001.

https://doi.org/10.5194/bg-2019-448
Preprint. Discussion started: 19 November 2019

Biogeosciences
Discussions
Open Access
EGU

502

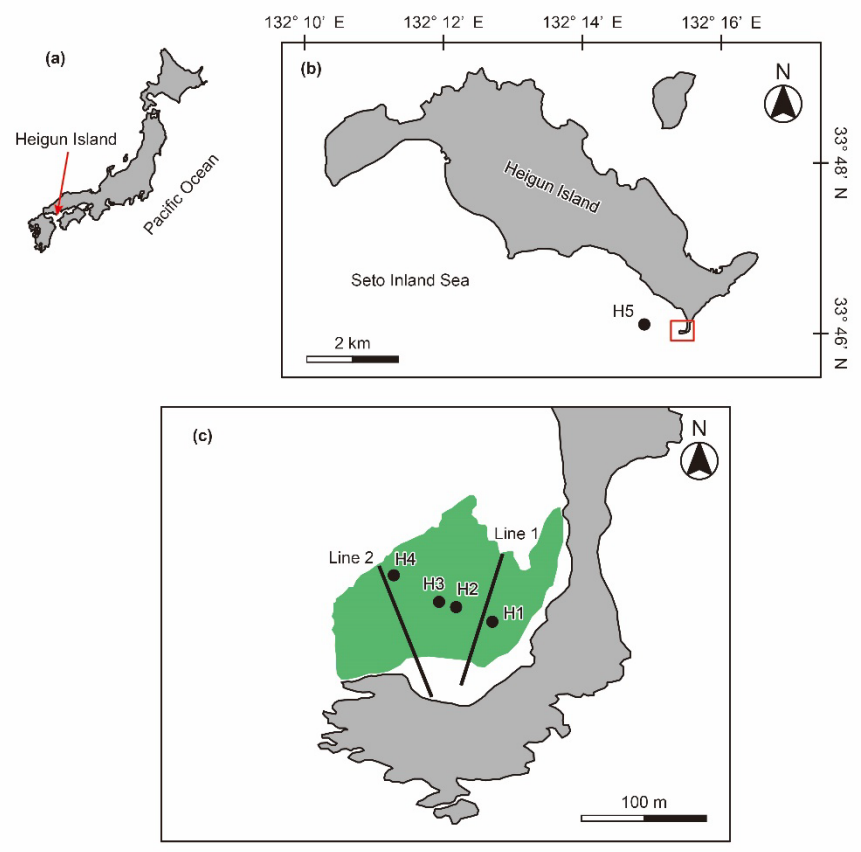

503

504 **Figure 1:** Maps of Heigun Island and the locations of sampling stations and transect lines. Green shading indicates the area occupied by a
505 macroalgal bed.

506

https://doi.org/10.5194/bg-2019-448
Preprint. Discussion started: 19 November 2019

Biogeosciences
Discussions
Open Access
EGU

507

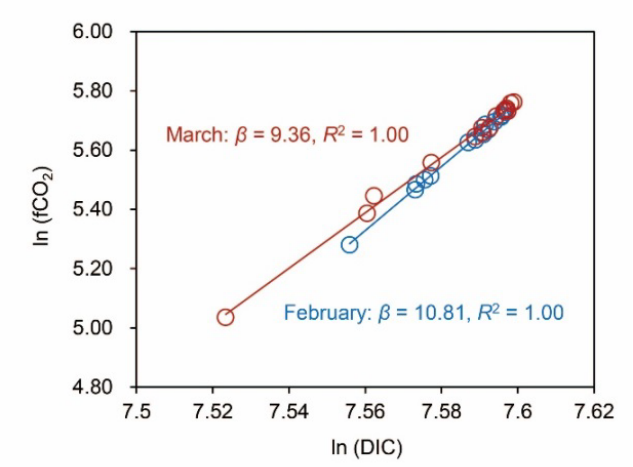

508
509 **Figure 2:** Plots of fugacity of CO_2 (fCO_2) versus dissolved inorganic carbon (DIC) and regression lines to determine the homogeneous
510 buffer factors (β) as slopes.

511

https://doi.org/10.5194/bg-2019-448
Preprint. Discussion started: 19 November 2019

512

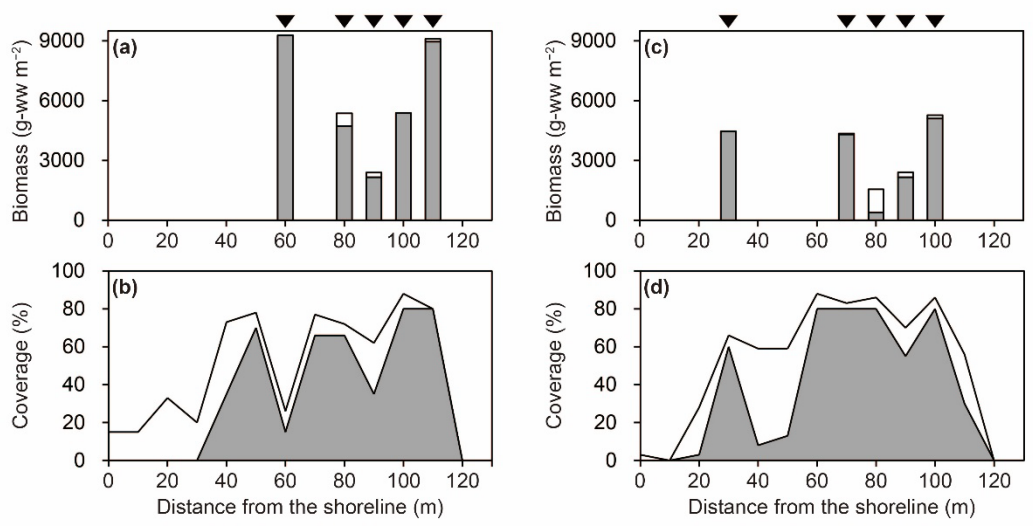

513
514 **Figure 3:** Biomass and coverage of macroalgae along transect line 1 (a, b) and line 2 (c, d) in March 2019. Grey and white shading
515 indicate sargassaceous algae and other macroalgae, respectively. Black arrows indicate sampling locations for macroalgal biomass.

516

https://doi.org/10.5194/bg-2019-448
Preprint. Discussion started: 19 November 2019

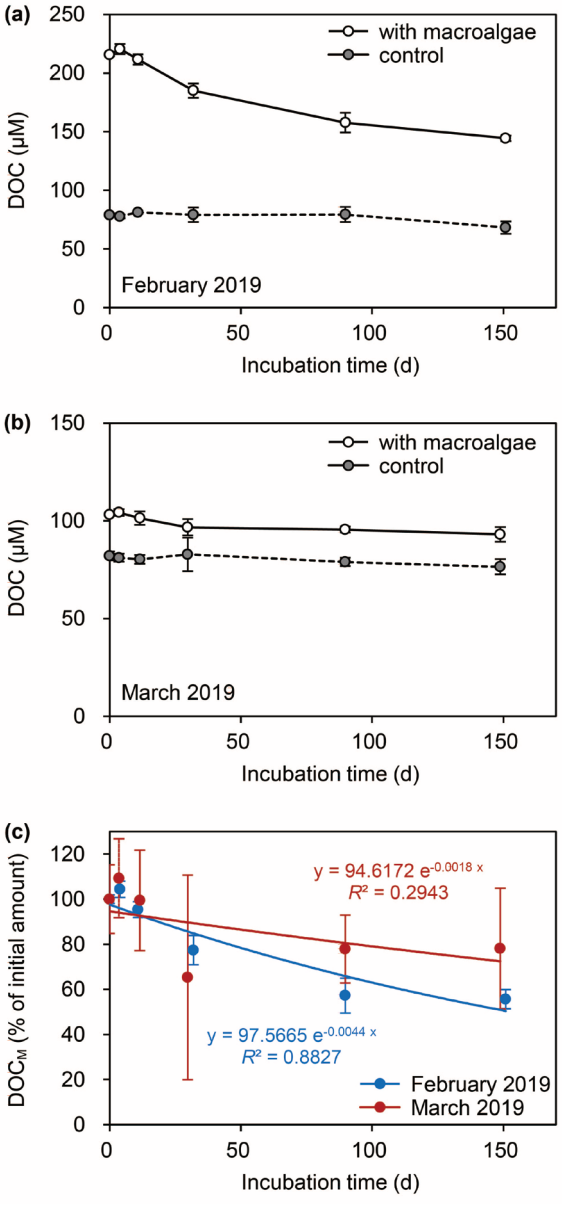

Figure 4: Time course of dissolved organic carbon (DOC) during the degradation experiments. DOC_M is DOC derived from macroalgae. Error bars show standard deviations.

https://doi.org/10.5194/bg-2019-448
Preprint. Discussion started: 19 November 2019

522

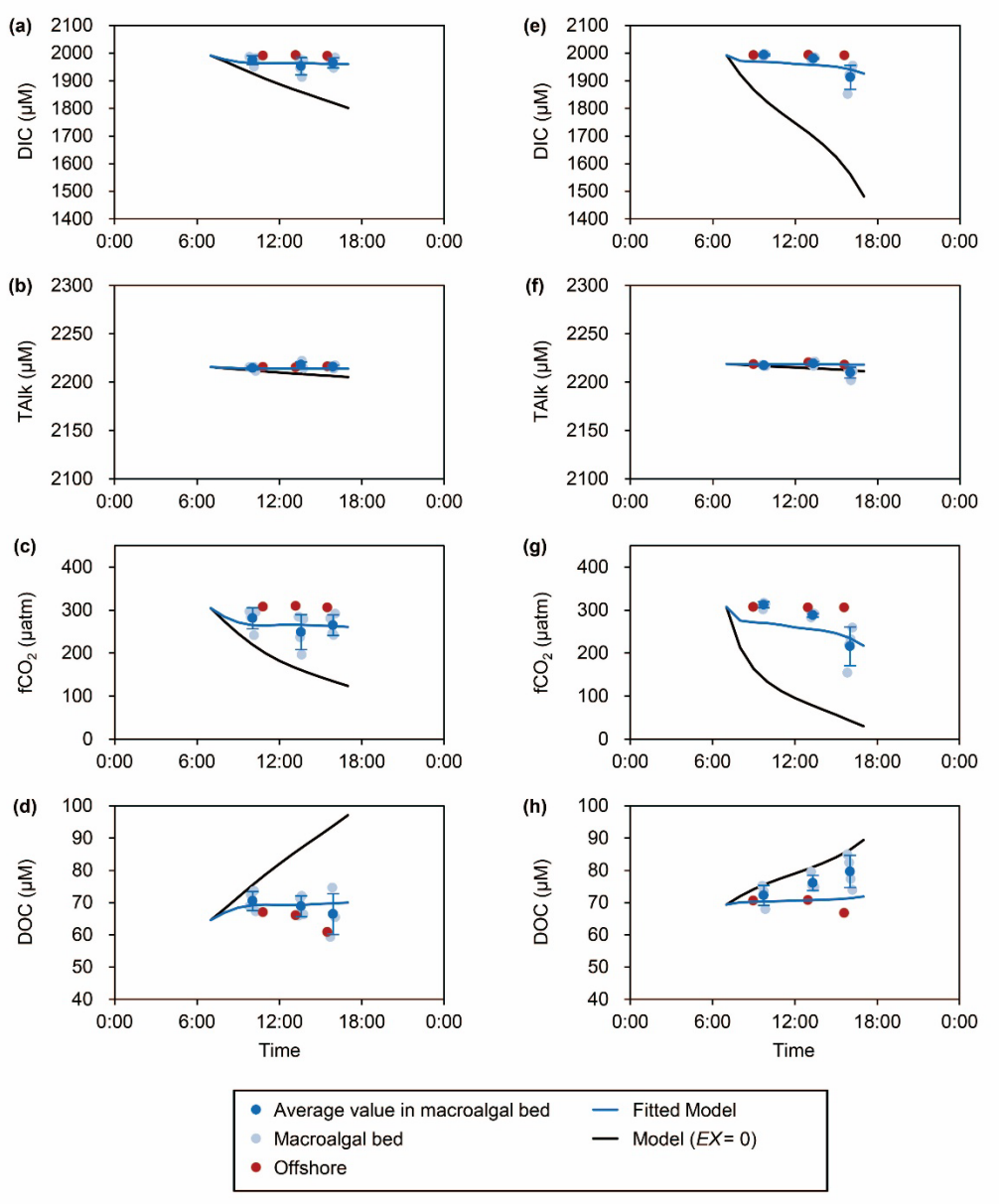

523
524 **Figure 5:** Temporal changes in dissolved inorganic carbon (DIC), total alkalinity (TAlk), fugacity of CO_2 (fCO_2), and dissolved organic
525 carbon (DOC) in February (a–d) and March (e–h). Modelled values of chemical parameters were estimated by using mass balance models.
526 Error bars show standard deviations. Black lines show the model results if the water exchange rates (*EX*) are zero.

527

https://doi.org/10.5194/bg-2019-448
Preprint. Discussion started: 19 November 2019

528

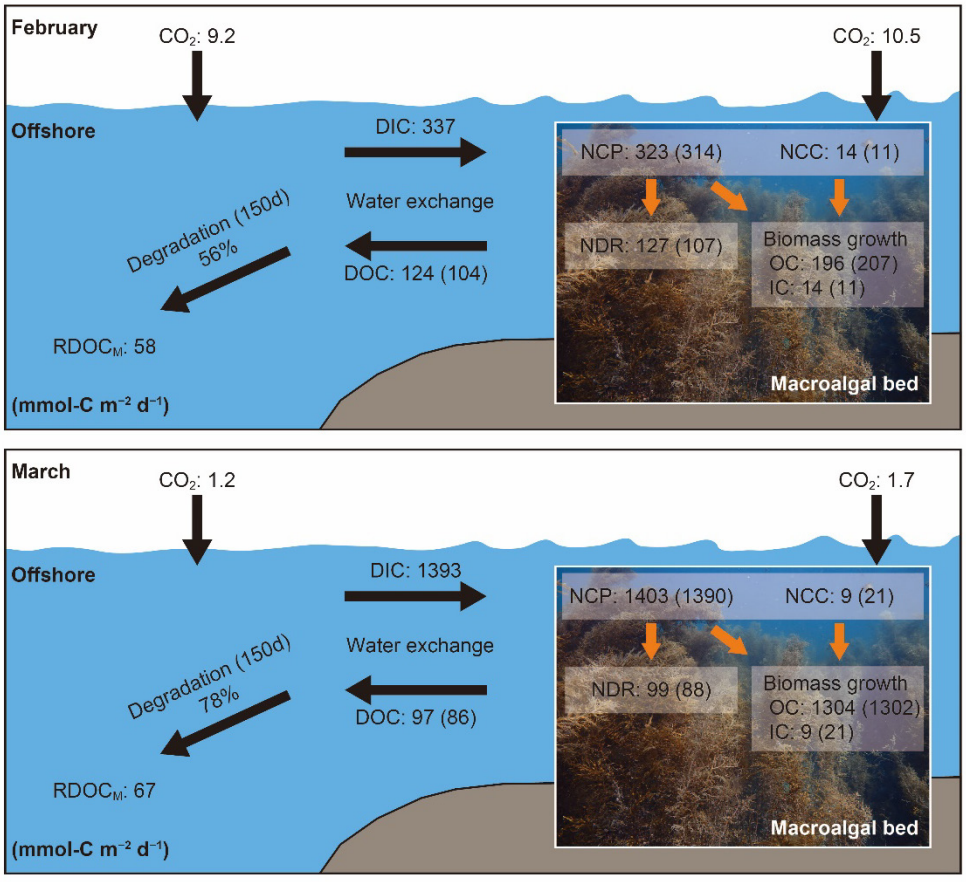

529
530 **Figure 6:** Carbon flows and community metabolism (NCP, net community production; NCC, net community calcification; NDR, net DOC
531 release) in the macroalgal bed. The parentheses show the carbon flows due to macroalgae. Biomass growth in terms of organic carbon was
532 calculated by subtracting NDR from NCP. Carbon fluxes were calculated in units of mmoles per square metre of the surface area of the
533 macroalgal bed per day.

534

https://doi.org/10.5194/bg-2019-448
Preprint. Discussion started: 19 November 2019

Biogeosciences Discussions Open Access EGU

535

536 **Table 1:** Salinity, dissolved inorganic carbon (DIC), total alkalinity (TAlk), fugacity of CO_2 (fCO_2), and dissolved organic
537 carbon (DOC) in the surface layer of the macroalgal bed and the offshore site. Mean ± standard deviation and the range of
538 each variable are shown.
539

Survey and site	Salinity	DIC (μmol L^{-1})	TAlk (μmol L^{-1})	fCO_2 (μatm)	DOC (μmol L^{-1})
February 2019					
Macroalgal bed (n = 12)	33.6 ± 0.1 (33.6–33.7)	1964 ± 22 (1912–1986)	2216 ± 3 (2211–2222)	265 ± 31 (196–298)	68.6 ± 4.4 (59.3–74.6)
Offshore (n = 3)	33.6 ± 0.1 (33.6–33.7)	1991 ± 1 (1990–1992)	2216 ± 0 (2215–2216)	305 ± 3 (302–307)	64.6 ± 3.3 (60.8–67.0)
March 2019					
Macroalgal bed (n = 12)	33.5 ± 0.1 (33.5–33.7)	1962 ± 43 (1851–1996)	2215 ± 5 (2202–2221)	272 ± 49 (154–318)	76.0 ± 4.6 (67.9–84.9)
Offshore (n = 3)	33.5 ± 0.0 (33.5–33.6)	1992 ± 1 (1991–1993)	2219 ± 1 (2218–2220)	309 ± 1 (308–310)	69.3 ± 2.3 (66.7–70.7)

540

541

https://doi.org/10.5194/bg-2019-448
Preprint. Discussion started: 19 November 2019

542

543 **Table 2:** Carbon metabolism, surface water temperature, photosynthetic photon flux, day length, and chlorophyll
544 fluorescence on February and March 2019. For macroalgae, mean ± standard deviation are shown. Average water depth and
545 biomass in the bed were used for calculating metabolic rates.
546

Variables	Units	February 2019	March 2019
Macroalgae			
Net community production	mmol-C m^{-2} d^{-1}	314 ± 131	1390 ± 643
Gross community production	mmol-C m^{-2} d^{-1}	583 ± 130	1657 ± 632
Community respiration	mmol-C m^{-2} d^{-1}	269 ± 12	267 ± 114
Net DOC release	mmol-C m^{-2} d^{-1}	107 ± 36	88 ± 37
Net community calcification	mmol-C m^{-2} d^{-1}	11 ± 7	21 ± 23
Control (phytoplankton)			
Net community production	mmol-C m^{-2} d^{-1}	9	13
Gross community production	mmol-C m^{-2} d^{-1}	23	23
Community respiration	mmol-C m^{-2} d^{-1}	14	10
Net DOC release	mmol-C m^{-2} d^{-1}	20	11
Net community calcification	mmol-C m^{-2} d^{-1}	3	−12
Surface water temperature	°C	12.0 ± 0.2	12.4 ± 0.1
Photosynthetic photon flux	µmol m^{-2} s^{-1}	674 ± 595	1311 ± 202
Day length	h	11	12.5
Chlorophyll fluorescence	µg L^{-1}	0.3	0.8

547

548

https://doi.org/10.5194/bg-2019-448
Preprint. Discussion started: 19 November 2019

549

550 **Table 3:** Water exchange rates (EX_r *and* EX_{tide}), FCO_2, DIC exchange, and DOC exchange, which were estimated by using
551 mass balance models. Carbon fluxes were calculated as mmoles per square metre of the surface area of the algal bed per day.
552

Variables	Units	February 2019	March 2019
EX_r	% h^{-1}	35	50
EX_{tide}	% h^{-1}	0–13	0–26
FCO_2 in macroalgal bed	mmol-C m^{-2} d^{-1}	10.5	1.7
FCO_2 in offshore	mmol-C m^{-2} d^{-1}	9.2	1.2
DIC exchange	mmol-C m^{-2} d^{-1}	337	1393
DOC exchange	mmol-C m^{-2} d^{-1}	−124	−97

553

554